Egypt. J. Chem. **Vol. 61**, No. 6, pp. 1073 - 1081 (2018)

Structural and Optical Properties of Wet-chemistry Cu co-doped $ZnTiO_3$ Thin Films Deposited by Spin Coating Method

Amany M. El Nahrawy[1*], Ahmed I. Ali[2], Ali B. Abou Hammad[1], Aïcha Mbarek[3]
[1]Solid State Physics Department, Physics Research Division, National Research Centre (NRC)-33 El Bohouth St. Dokki, P.O.12622, Egypt. (Affiliation ID:60014618)
[2]Basic Science Department, Faculty of Industrial Education & Technology, Helwan University, Cairo, 11281, Egypt.
[3]Laboratory of Advanced Materials, National Engineering School, University of Sfax, BP 1173- 3038 Sfax-Tunisia.

$Zn_{1-x}TiO_3$:xCu (x=0%, 1%, 5%) thin films were prepared on glass and quartz substrates via the sol-gel method (wet-chemistry) and spin coating process. Structural and optical properties of the prepared films have been characterized by X-ray diffraction, field emission scanning electron microscope and UV-visible spectrophotometer. The doping of the thin films by different concentration of Cu ions exhibited change in structure from cubic to hexagonal system. The average crystalline size was calculated from X-ray line broadening and it is decreased from 21.88 nm ($ZnTiO_3$) to 11.21 nm ($Zn_{0.95}Cu_{0.05}TiO_3$). The fundamental optical constants of the thin films (refractive index, absorption coefficient, extinction coefficient, dielectric constant, band gap) were determined using the UV-Vis reflectance and transmittance spectroscopy. The analysis of the optical absorption data revealed that undoped film has indirect transition (E_g = 3.22 eV) and the Cu-doped films have direct allowed transition with band gap energy increased to 3.96 eV.

Keywords: $ZnTiO_3$ perovskite, Cu doping, Sol-gel method (wet-chemistry), Optical properties.

Introduction

Perovskite-type titanates with the general formula $MTiO_3$ (M is a alkali earth or transition metals) have attracted much attention for the important technological applications in the electronics industry, due to their excellent inherent chemical and physical properties such as photoelectricity, photorefractivity, ferroelectricity, as well as high dielectric constant [1-3]. Particularly, Zinc titanate $ZnTiO_3$ nanostructures have been an active area of research because of their remarkable electrical properties leading to the wide practical applications in microwave resonator, gas sensors, microelectronics and photocatalytic [4-6]. More interest has been given to probe the optical and electrical properties of Zinc titanates by doping with some transition metal ions [7–10]. Kim *et al.* and other researchers [7-10] tried to obtain suitable dielectric properties by controlling composition in $Zn_xMg_{1-x}TiO_3$ and $Zn_xCo_{1-x}TiO_3$ systems.

Doped or undoped $ZnTiO_3$ films can be prepared by many techniques such as RF magnetron sputtering pulsed laser deposition and the sol-gel method [11-13]. Among them, the sol-gel method is preferred for several advantages, such as producing good quality nano-crystalline films, low processing temperature, possibility of deposition of films of small as well as large areas and complicated forms on various substrates and most important cost effective [14-16].

In present work, undoped and Cu-doped $ZnTiO_3$ thin films were prepared on glass and quartz substrates by sol-gel method followed by spin coating process in order to study their optical properties. The structural characteristics of samples were analyzed by X-ray diffraction (XRD) as well as Raman spectroscopy, whereas

*Corresponding author e-mail: amany_physics_1980@yahoo.com
DOI: 10.21608/ejchem.2018.4069.1359

the thickness and surface morphology of the thin films were observed by field emission scanning electron microscope (FE-SEM). Furthermore, the optical constants of the prepared films were investigated for obtained optical band gap, refractive index, extinction coefficient, dielectric constant and dispersion parameters.

Experimental

Samples preparation

The $Zn_{1-x}TiO_3$:xCu (x = 0%, 1%, 5%) nanocrystallines were synthesized by sol-gel process using Zinc acetate $Zn(CH_3COO)$, Titanium(IV) n-butoxide, Diethanolamine and Nitric acid. The TiO_2 sol was prepared by dissolving Titanium(IV) n-butoxide into absolute ethanol (C_2H_5OH) and stirred vigorously for 2 h, to prepare a clear solution. Zinc acetate was dissolved in distilled water with drops of nitric acid and ethanol, then mixed with TiO_2 sol and diethanolamine under vigorous stirring for 2 h. For $Zn_{0.99}Cu_{0.01}TiO_3$ and $Zn_{0.95}Cu_{0.05}TiO_3$ samples, copper nitrate was first dissolved in distilled water and mixed with Zinc sol before added to TiO_2 sol. $ZnTiO_3$ and $Zn_{1-x}Cu_xTiO_3$ (x = 0.01, 0.05) thin films were prepared by depositing the respective sols on glass and quartz substrates ($2x1cm^2$) using spin-coating technique and were annealed at 400°C and 600 °C for 1 hour. Three successive layers were deposited on glass substrates for optical measurements and five successive layers deposited on quartz substrates for structural measurements.

Samples Characterization

The phase and structure of the deposited films were identified at room temperature using an X-ray diffractometer model RAD IIA, with CuK_α radiation ($\lambda = 0.15418$ nm). The lattice parameters were calculated from θ−2θ patterns. Raman spectra were performed at room temperature with a Olympus BX40 spectrometer. Excitation at 514.5 nm was supplied with a Spectra Physics 8 mW argon laser. The thickness and surface morphology of pure and Cu-doped $ZnTiO_3$ thin films were observed by field emission scanning electron microscope (FE-SEM, FEI Quanta FEG-250), the thickness as measured by a cross-sectional view of FE-SEM were between 250, 276, and 300 nm for $ZnTiO_3$, $Zn_{0.99}Cu_{0.01}TiO_3$ and $Zn_{0.95}Cu_{0.05}TiO_3$ thin films, respectively. The optical transmission and reflection spectra were measured using UV/Vis double-beam spectrophotometer (Cary 5E) in the wavelength range of 200 to 800 nm. The optical parameters such as, optical energy gap, refractive index, extinction coefficient, dielectric constant (real and imaginary parts), oscillator energy (E_0), dispersion energy (E_d), optical conductivity (real and imaginary parts), volume energy loss (*VEL*), surface energy loss (*SEL*) were estimated.

Results and Discussion

The XRD patterns of $Zn_{1-x}Cu_xTiO_3$ (x = 0, 0.01, 0.05) thin films are shown in Fig.1. It is observed that all of the diffraction peaks for undoped film, were assigned to the cubic $ZnTiO_3$ phase with lattice constants: $a = b = 8.4449$ Å (JCPDS N°. 99-101-2657). While, the patterns of both $Zn_{0.99}Cu_{0.01}TiO_3$ and $Zn_{0.95}Cu_{0.05}TiO_3$ thin films were assigned to the hexagonal $ZnTiO_3$ phase (JCPDS N°. 14-0033). From Table 1, it is observed that the lattice parameters do not change significantly between the two Cu-doped samples, indicating that doping of Cu^{2+} ion in host matrix do not cause any significant structural change in the investigated concentration range.

The average crystallite size was determined from the XRD powder pattern according to the Scherrer's equation [17]:

$$D = \frac{k\lambda}{(\beta \cos\theta)} \quad (1)$$

where D is the average grain size, k is a constant equal to 0.9, λ is the X-ray wavelength (0.1542 nm), β is full width at half maximum, and θ is diffraction angle. The average grain sizes of $ZnTiO_3$, $Zn_{0.99}Cu_{0.01}TiO_3$ and $Zn_{0.95}Cu_{0.05}TiO_3$ films were about 21.88, 15.25, and 11.21 nm, respectively. Noting that the average grain sizes of $ZnTiO_3$ films decrease dramatically on increasing the Cu dopant content.

Figure 2 displays the Raman spectra of $ZnTiO_3$ and $Zn_{1-x}Cu_xTiO_3$ (x = 0.01, 0.05) films in the range 200-1000 cm^{-1}. The weak bands at 307, 351, 445 and 475 cm^{-1} are assigned to the oxygen vibration of Zn–O–Zn and Zn–O–Ti linkage in the perovskite network [18, 19]. The vibration modes at 445 cm^{-1} and 611 cm^{-1} is probably an indication of the dopant incorporated in $ZnTiO_3$ matrix. The band appeared in doped samples at 611 cm^{-1} corresponds to vibrations of Ti–O–Ti and Ti–O–Cu in the $ZnTiO_3$ framework. The most intensive bands at 307 cm^{-1} and 723 cm^{-1} are corresponding to the formation of polycrystallines $ZnTiO_3$ and $ZnTiO_3$: Cu with only very low oxygen vacancy [18, 19].

TABLE 1.The average particles sizes, lattice paramters of $ZnTiO_3$, $Zn_{0.99}Cu_{0.01}TiO_3$ and $Zn_{0.95}Cu_{0.05}TiO_3$ thin films with thickness 421, 452 and 492 nm, respectively, annealed at 600 °C for 1 h.

Sample	Average grain size (nm)	Average thickness (nm)	Lattice parameter (Å)	
$ZnTiO_3$	21.88±0.44	421± 2.11	a = 8.445	
$Zn_{0.99}Cu_{0.01}TiO_3$	15.25±0.31	452± 2.26	a = 5.072	c = 13.89
$Zn_{0.95}Cu_{0.05}TiO_3$	11.21±0.22	492± 2.46	a = 5.081	c =13.93

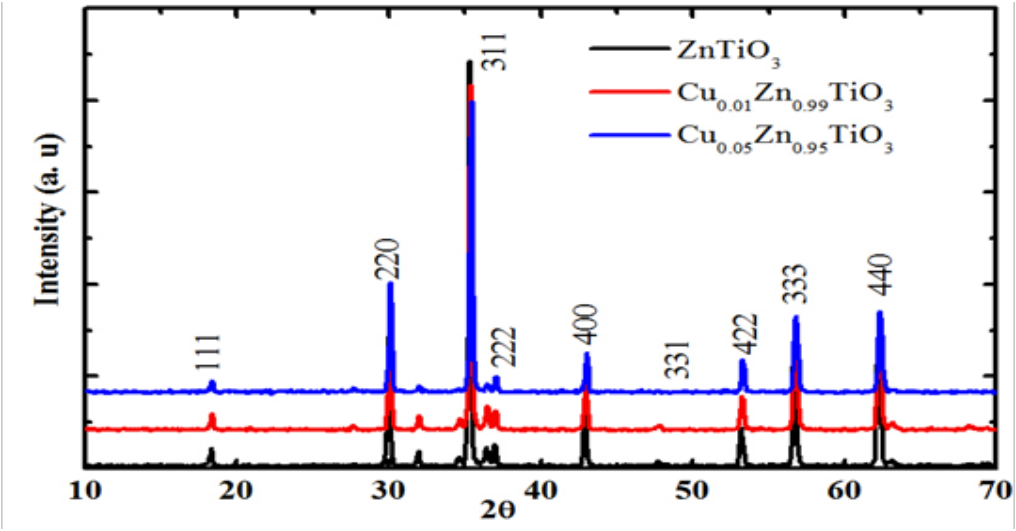

Fig. 1. XRD pattern of $Zn_{1-x}Cu_xTiO_3$ (x = 0%, 1%, 5%) thin films deposited on quartz substrates, annealed at 600 °C for 1 h.

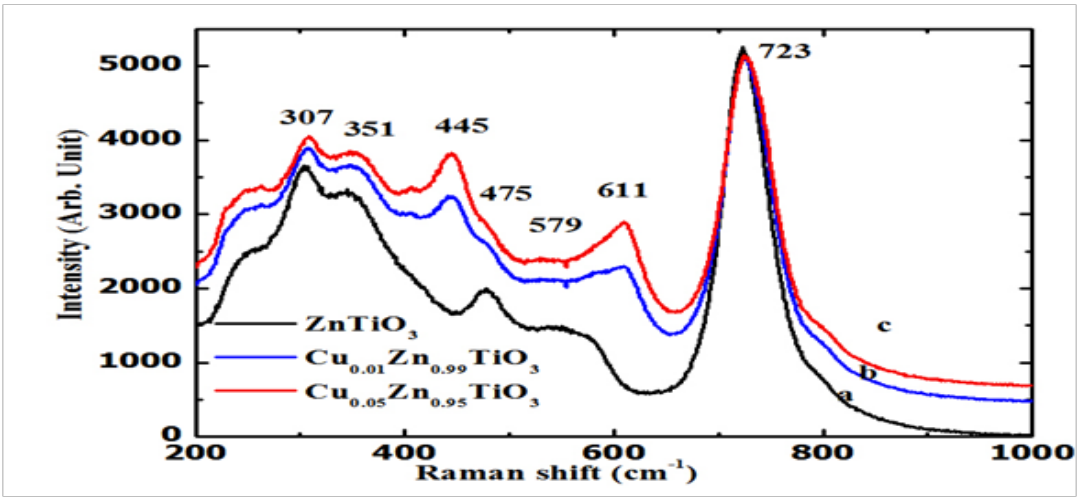

Fig. 2. Raman shift of thin films (a) $ZnTiO_3$ doped with two different concentrations of Cu ions (b)1 and (c) 5 mol% deposited on quartz substrates and annealed at 600 °C for 1 h.

Figure 3 shows the FE-SEM images of the $ZnTiO_3$ (Fig. 3a) and $Cu_{0.05}Zn_{0.95}TiO_3$ (Fig. 3b) thin films. It is clear that, the deposited films are polycrystallines in nano-size particles. Moreover, the grain size is around 10~20 nm and the thickness equal 250~300 nm for films. All films present different surface morphologies reflecting their strains of substrates. Thus, the grain size of undoped $ZnTiO_3$ film is larger than those of 5%Cu-doped $ZnTiO_3$, which also indicates that the doping of Cu suppresses the growth of grains.

Figure 4(a) and (b) show the optical transmission and reflection as a function of wavelength for $ZnTiO_3$, $Zn_{0.99}Cu_{0.01}TiO_3$ and $Zn_{0.95}Cu_{0.05}TiO_3$ thin films. Both doped samples have the highest transmittance compared with the $ZnTiO_3$ thin film. The transmittance values of Cu-doped films increased up to the double of its value of $ZnTiO_3$ film. In addition, $Zn_{0.99}Cu_{0.01}TiO_3$ and $Zn_{0.95}Cu_{0.05}TiO_3$ films have a similar behavior of transmittance. Whilst, the $ZnTiO_3$ thin film has the lowest reflection at lower wavelengths compared with Cu-doped thin films.

Figure 4(c) shows the absorption coefficient (α) as a function of photon energy of the $Zn_{1-x}TiO_3$:xCu (x = 0%, 1%, 5%) thin films evaluated from the transmittance and reflection spectra as the following equation [20]:

$$\alpha = (\frac{1}{d}) \ln(\frac{(1-R)^2}{T}) \quad (2)$$

where d is the film thickness, R is the reflectance of the studied films and T is the transmittance of these films. The optical energy gaps (E_g) were determined from the optical absorption curves using the imperial equation [20]:

$$\alpha = A(h\nu - E_g)^p \quad (3)$$

where A is a constant, v is the frequency of the incident radiation and h is the Planck's constant. It is known that, the exponent $p = 1/2$ for allowed direct transition, while $p = 2$ for allowed indirect transition. Plotting $(\alpha h\nu)^2$ against photon energy ($h\nu$) gives a straight line with intercept equal to the optical energy band gap for direct transitions as shown in Fig. 4(d). The $ZnTiO_3$ film has indirect energy gap (E_g^{ind}) with the value 3.22 eV and the Cu-doped $ZnTiO_3$ films have a direct energy gaps (E_g^{dir}) and were found to be 3.92 for $Zn_{0.99}Cu_{0.01}TiO_3$ and 3.96 eV for $Zn_{0.95}Cu_{0.05}TiO_3$ film. This means that the kind of doping plays an important rule in the change optical energy gap for the investigated films from indirect to direct transitions. It seems the Cu level has the same effect for the energy gap of the $ZnTiO_3$ thin film and the type of transition is depending on the type (ionic radius) of the doping element. The extinction coefficients for the prepared films were evaluated using the relation:

$$k = \frac{\alpha \cdot \lambda}{4\pi} \quad (4)$$

Figure 5(a) presented the relation between extinction coefficients of $Zn_{1-x}TiO_3$:xCu (x = 0%, 1%, 5%) and the photon energy. It can be noticed that the extinction coefficient of the $ZnTiO_3$ thin film has the same behavior absorption. Then, an important decrease of the extinction coefficient values is clearly observed for the doped films.

Figure 5(b) shows the plot of refractive index (n) versus energies (eV) of $ZnTiO_3$ and $ZnTiO_3$: Cu films. Refractive index was calculated using the following equation [21]:

$$n = \frac{(1+\sqrt{R})}{(1-\sqrt{R})} \quad (5)$$

where R is the reflectance. It could be seen that $ZnTiO_3$ film had the highest refractive index (1.4 ~1.6) at lower energies (E < 2.5 eV) and the refractive index decreased gradually to less than 1.2 at higher photon energies (E > 4 eV), while the $Zn_{0.99}Cu_{0.01}TiO_3$ and $Zn_{0.95}Cu_{0.05}TiO_3$ films have the same value of the refractive index with little change around energy of 3.5 eV, there is a sudden decrease to the value of 1.4, which is similar to the behavior of the reflectance spectra too. The dispersion of refractive index in $ZnTiO_3$ and Cu-doped $ZnTiO_3$ thin films was analyzed using the concept of the single oscillator and can be expressed by the Wemple–DiDomenico relationship [22]:

$$n^2(E) - 1 = \frac{E_o E_d}{{E_o}^2 - E^2} \quad (6)$$

where $E = h\nu$ is the photon energy, E_o is the oscillator energy and E_d is the dispersion energy. The values of E_o and E_d are obtained from the intercept and the slope resulting from the extrapolation of the lines in Fig. 5(d). The calculated values of E_o and E_d for all samples are summarized in Table 2. Figure 5(c) and (d) show the relation between (refractive index)^2

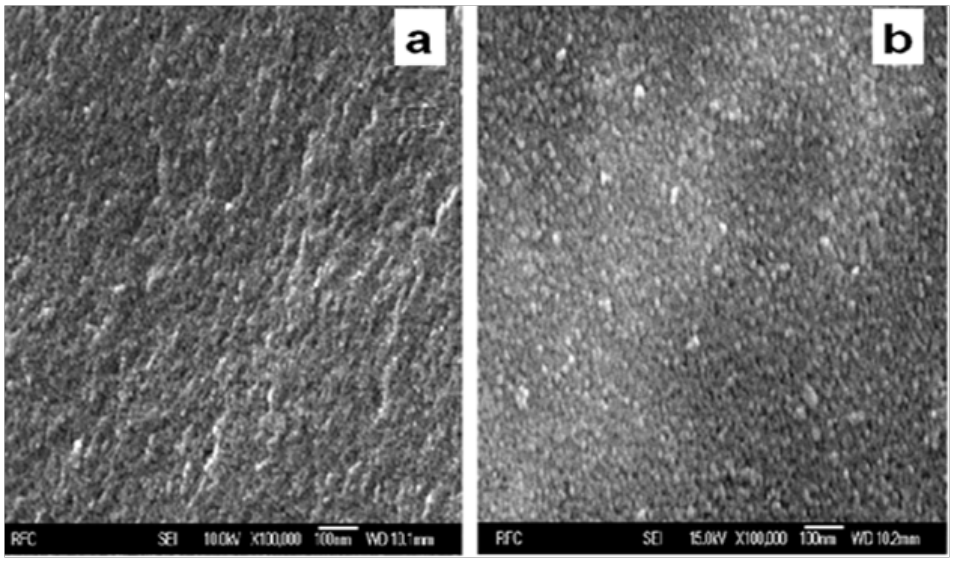

Fig. 3. FE-SEM images of the $ZnTiO_3$ and $Zn_{0.95}Cu_{0.05}TiO_3$ thin films deposited on quartz substrates and annealed at 600°C for 1 h.

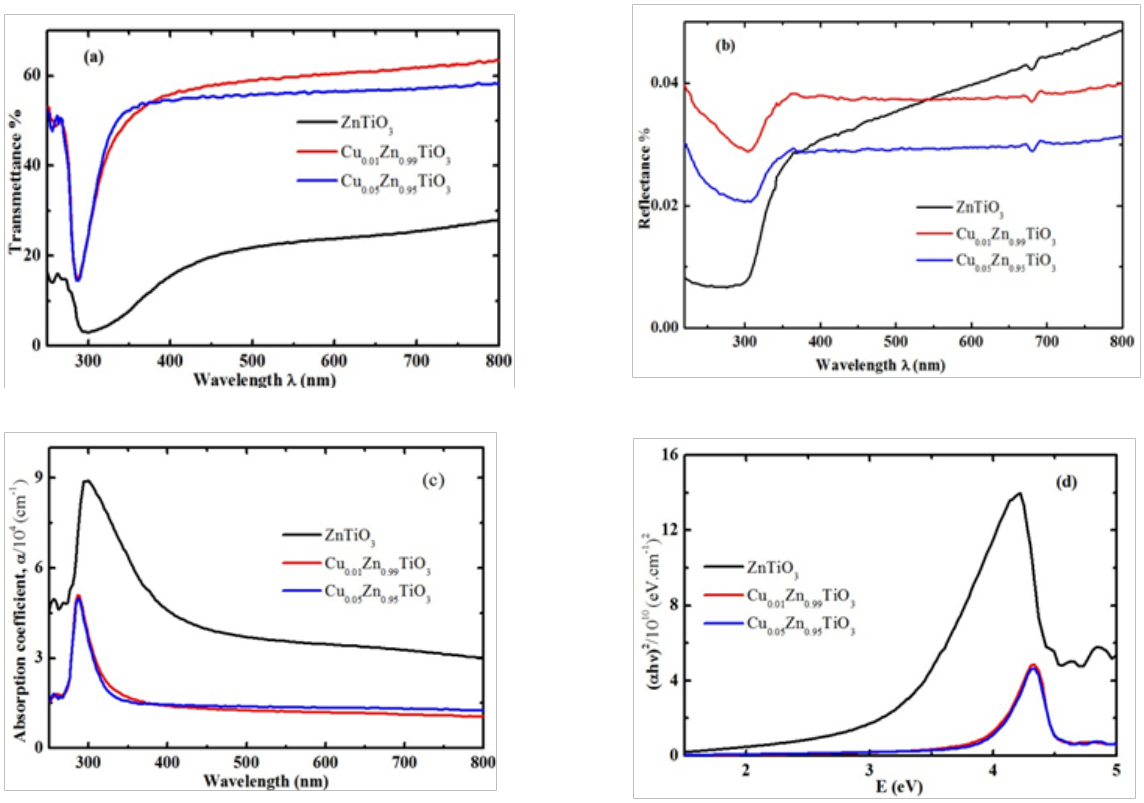

Fig. 4. (a) Transmittance, (b) Reflectance, and (c) Absorption coefficient as functions of wavelength. (d) $(\alpha h\nu)^2$ as a function of photon energy for $ZnTiO_3$, $Zn_{0.99}Cu_{0.01}TiO_3$ and $Zn_{0.95}Cu_{0.05}TiO_3$ thin films with thickness 250, 276 and 300 nm, respectively, deposited on glass substrates and annealed at 400 °C for 1 h.

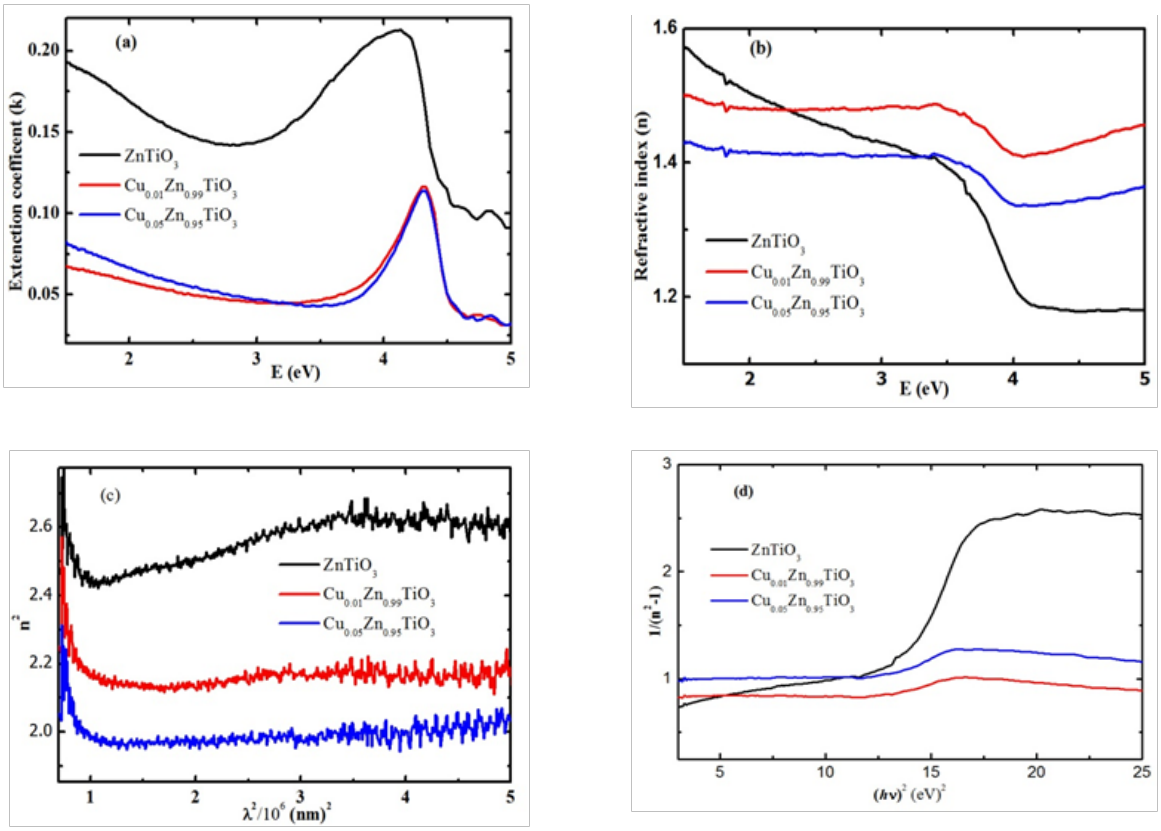

Fig. 5. (a) Extinction coefficient and (b) Refractive index as functions of wavelength. (c) n^2 as a function of square wavelength. (d) $1/(n-1)^2$ as a function of square photon energy for $ZnTiO_3$, $Cu_{0.01}Zn_{0.99}TiO_3$ and $Cu_{0.05}Zn_{0.95}TiO_3$ thin films with thickness 250, 276, and 300 nm, respectively, deposited on glass substrates and annealed at 400 °C for 1 h.

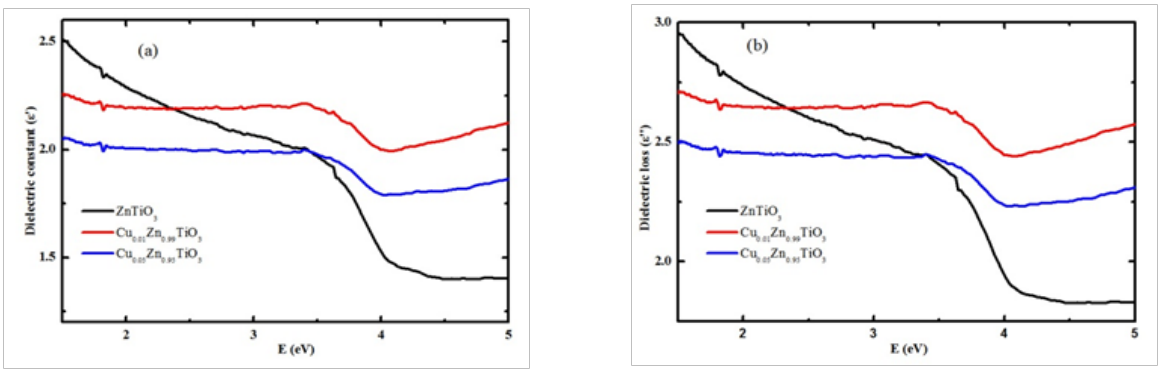

Fig. 6. (a) Real part, (b) Imaginary part of dielectric constant as a function of photon energy for $ZnTiO_3$, $Cu_{0.01}Zn_{0.99}TiO_3$, and $Cu_{0.05}Zn_{0.95}TiO_3$ thin films.

TABLE 2. The optical parameters of $ZnTiO_3$, $Zn_{0.99}Cu_{0.01}TiO_3$ and $Zn_{0.95}Cu_{0.05}TiO_3$ thin films with thickness 250, 276 and 300 nm, respectively, annealed at 400 °C for 1 h.

Sample	Desperation energy (E_d) (eV)	Oscillating energy (E_0) (eV)	Infinity Permittivity ε_∞	E_g (eV)	Average thickness (nm)	Type E_g
$ZnTiO_3$	0.47795	0.73	2.43	3.22	250.0± 1.25	Indirect
$Zn_{0.99}Cu_{0.01}TiO_3$	0.08885	0.82	2.17	3.92	276.0± 1.38	Direct
$Zn_{0.95}Cu_{0.05}TiO_3$	0.06468	0.99	1.99	3.96	300.0±1.50	Direct

and (wavelength)^2 for the $ZnTiO_3$ and Cu-doped $ZnTiO_3$ thin films. Table 2 shows that the dispersion energy E_d decreased, while the oscillator energy E_o increased with doping Cu ions into $ZnTiO_3$ films, reflecting the level of a Cu band between the valence band and the conduction band.

The dielectric constant is a fundamental property of the material and it affects the movement of the electromagnetic signals through the materials. The dielectric constant is a complex quantity and consists of a real part (*ε›*) which represents the storage and an imaginary part (*ε››*) which represents the loss. The dielectric parameters were determined using the obtained values of the refractive index (*n*) and the extinction coefficient (*k*) as in the following equations [23] :

$$\varepsilon' = (n^2 + k^2) \qquad (7)$$

$$\varepsilon'' = \left[(n^2 + k^2)^2 - (n^2 - k^2)^{0.5} \right] \qquad (8)$$

The dependences of *ε'* and *ε"* on photon energy for undoped and doped thin films are shown in Fig. 6 (a, b). It is seen that both *ε'* and *ε"* decreases with increasing wavelength. The real and imaginary parts follow the same pattern and the values of imaginary part are a little higher than the real parts. The presence of Cu activator causes important changes in real part and imaginary parts of the dielectric constant of the films.

Conclusion

In summary, $Zn_{1-x}Cu_xTiO_3$ (x = 0%, 1%, 5%) thin films have been deposited on glass and quartz substrates by the spin-coating method.The doping of Cu does change the cubic structure of $ZnTiO_3$ films. The grain sizes of $ZnTiO_3$ films decrease dramatically on increasing the Cu dopant content. The optical properties of the thin films have been investigated. The dependence of the optical constants (refractive index (*n*), extinction coefficient (*k*), dielectric constant (*ε*)) of undoped and Cu-doped films were studied. The normal dispersion of the refractive index of the films could be described using the Wemple–DiDomenico single oscillator method. $ZnTiO_3$ and Cu-doped $ZnTiO_3$ thin films on quartz substrates have respectively indirect and direct allowed transitions corresponding to the energy gap E_g^{ind} = 3.2 eV and E_g^{dir} = 3.9 eV. The dispersion and oscillating energy as well as effective mass for these films showed that, the increase of Cu rates affects the values of these calculated parameters.

References

1. Qin Y., Hu Z., Lim B.H., Yang B., Chong K.K., Chang W.S., Zhang P., Zhang H., Performance Improvement of Dye-Sensitized Solar Cell by Introducing Sm^{3+}/Y^{3+} Co-doped TiO_2 Film as an Efficient Blocking Layer, *Thin Solid Films,* **631**, 141-146 (2017).

2. Qian X., Gao Y. M., Cao Q. Y., Guo L. B., Li D. A., Preparation and phase structures of Zn–Ti–O ternary compounds by atomic layer deposition, *J of Vacuum Science & Technology A Vacuum Surfaces and Films*, **31**, A1331-A1336 (2013).

3. M. Rahimi-Nasrabadi, M. Behpour, A. Sobhani-Nasab, S.M. Hosseinpour-Mashkani, ZnFe 2− x

La x O 4 nanostructure: synthesis, characterization, and its magnetic properties, *J. Mater. Sci.,* **26,** 9776-9781(2015).

4. Song C. F., Qiu T., Yuan H. F., Li X.Y., Enhanced green emission in ZnO/zinc titanate composite materials, *Mater Sci Eng B,* **175**, 243–250 (2010).

5. Lee Y.C., Huang Y. L., Lee W. H., Shieu F. S, Formation and transformation of $ZnTiO_3$ prepared by sputtering process. *Thin Solid Films,* **518**, 7366-7371 (2010).

6. Liu X. C., Zhao M., Gao F., Zhao L. L., Tian C. S, Effects of WO_3 additions on the phase structure and transition of zinc titanate ceramics, *J . Alloys Compd*; **450**, 440-445 (2008).

7. Lokesh B., Rao M., Effect of Cu-doping on structural, optical and photoluminescence properties of zinc titanates synthesized by solid state reaction, *J. Mater Sci: Mater Electron*, **27**, 4253-4258 (2016).

8. Kim T. H., Lanagan T. M., Structure and microwave dielectric properties of $(Zn_{1-x}Co_x)TiO_3$ ceramics, *J. Am. Ceram. Soc.,* **86**, 1874-1878 (2003).

9. Liu X. Molten salt synthesis of $ZnTiO_3$ powders with around 100 nm grain size crystalline morphology, *Materials Letters*, **80**, 69-71 (2012).

10. Hsieh L. M., Chen S. L., Hsu C. H., Wang S., Houng P. M., Fu L. S., Effect of oxide additives on the low-temperature sintering of dielectrics (Zn, Mg)TiO_3, *Mater. Res. Bull.*, **43**, 3122-3129 (2008).

11. Jain K. P., Salim M., Kaur D., Effect of phase transformation on optical and dielectric properties, *Superlattices Microstruct,* **92**, 308-315 (2016).

12. Pal N., Paul M., Bhaumik A., New mesoporous perovskite $ZnTiO_3$ and its excellent catalytic activity in liquid phase organic transformations, *Applied Catalysis A: General*, **393**, 153–160 (2011).

13. Yang J., Swisher J. H., The phase stability of $Zn_2Ti_3O_8$, *Mater Charact*, **37**, 153–163 (1996).

14. Polychronopoulou K., Cabello Galisteo F., López Granados M., Fierro G. L. J., Bakas T., Efstathiou M. A., Novel Fe–Mn–Zn–Ti–O mixed-metal oxides for the low-temperature removal of H_2S from gas streams in the presence of H_2, CO_2, and H_2O, *Journal of Catalysis*, **236**, 205–220 (2005).

15. Wang L., Kang H., Xue D., Liu C., Low-temperature synthesis of $ZnTiO_3$ nanopowders, *Journal of Crystal Growth,* **311**, 611-614 (2009).

16. A. M. El Nahrawy M. A., Structural studies of sol gel prepared nano-crystalline silica zinc titanate ceramic, *International Journal of Advancement in Engineering, Technology and Computer Sciences, IJAETC,* **2**, 15-18 (2015).

17. El Nahrawy M. A., Soliman A. A., Mosa M. W., Salah El-Deen H., Synthesis and magnetic properties of $Al_{0.3}Ni_{0.2}Zn_{0.5}Fe_2O_4$ nanocrystalline prepared by sol gel process, *IJAETCS,* **4**, 5-9 (2017).

18. Hou L., Hou D-Y., Zhu K. M., Tang J., Liu B. J., Wang H., Yan H, Formation and transformation of ZnTiO3 prepared by sol–gel process, *Materials Letter*s, **59**, 197-200 (2005).

19. Periyat P., Ullattil S.G., Sol–gel derived nanocrystalline ZnO photoanode filmfordye sensitized solar cells, *Materials Science in Semicon. Proces.*, **31**, 139-146 (2015).

20. Fadel M., Fayek A. S., Abou-Helal O. M., Ibrahium M. M., Shakra M. A., Structural and Optical Properties of SeGe and $SeGe_X$ (X = In, Sb and Bi) Amorphous Films, *J. Alloys Compd.*, **485**, 604-609 (2009).

21. Pankove I. J., *Optical Process in Semiconductors,* Prentice-Hall, Inc., (1971).

22. Torres J., Cisneros I. J., Gordillo G., Alvarez F., A simple method to determine the optical constants and thicknesses of $Zn_xCd_{1-x}S$ thin films, *Thin Solid Films*, **289**, 238-241(1996).

23. Sze M. S., *Physics of Semiconductor Devices.* Wiley-Interscience, New York, (1981).

(Received 8/6/2018;
accepted 30/7/2018)

الخواص التركيبية والضوئية لافلام النحاس-زنك تيتانات والمرسبة بطريقة التغطية المغزلية للسائل الجيلاتينى

أمانى محمد النحراوى[١], احمد على[٢] ,على ابوحماد[١], عائشة مبارك[٣]
[١]قسم فيزياء الجوامد - المركز القومى للبحوث - الجيزة - مصر.
[٢]قسم علوم المواد - كلية التعليم الصناعى – جامعة حلوان - مصر.
[٣]قسم المواد المتقدمة - جامعة صفاقص - تونس.

الأفلام الرقيقية للزنك تيتانات المطعمة بتركيزات مختلفة من النحاس و المحضرة طريقة السائل الجيلاتينى على شرائح زجاج وكوارتز.اختبرت الخواص التركيبية والضوئية باستخدام كل من اشعة الحيود السينى, الميكروسكوب الالكترونى الماسح و الميكروسكوب الضوئ. و أظهرت النتائج تكون المادة فى طور المكعب للسداسى تحت تاثير زيادة ايونات النحاس. تغير الحجم الذرى من ٢١,٨٨ نانومتر الى ١١,٢١ نانومتر. أظهرت الخواص الضوئية زيادة قيمة فجوة الحزمة لافلام الزنك تيتانات المطعمة بالنحاس من ٣,٢٢ الى ٣,٩٦ الكترون فولت.